Interband absorption in quantum wires. II. Nonzero-magnetic-field case

U. Bockelmann
Laboratoire de Physique de la Matière Condensée de l'Ecole Normale Supérieure, 24 rue Lhomond, F-75005 Paris, France and Walter Schottky Institut der TU München, Am Coulombwall, D-8046 Garching, Germany

G. Bastard
Laboratoire de Physique de la Matière Condensée de l'Ecole Normale Supérieure, 24 rue Lhomond, F-75005 Paris, France
(Received 13 March 1991)

We theoretically investigate a two-dimensional semiconductor system subjected to a periodic modulation in one lateral direction in a perpendicular magnetic field. Both type-I and type-II lateral superlattices are considered. The conduction and valence subbands as well as the polarization-dependent interband absorption are studied as a function of the strength V_1 of the lateral modulation. With increasing V_1, the optical transitions become increasingly anisotropic with respect to a polarization in the two-dimensional plane. Just as the calculated changes in the shape of the absorption spectrum, this reflects the continuous transition from a quasi-zero-dimensional characteristic to a quasi-one-dimensional characteristic of the electronic structure in the presence of a magnetic field.

The present second part of our discussion of the interband absorption in quasi-one-dimensional (1D) semiconductor structures deals with the influence of a constant magnetic field. In the first part [U. Bockelmann and G. Bastard, preceding paper, Phys. Rev. B **45**, 1688 (1992)], in the following labeled I, we have developed the theoretical framework and have applied it to different 1D structures at zero magnetic field.[1] A particular emphasis has been put on the influence of the light polarization in the lateral (xy) plane. It depends characteristically on the hh-lh mixing in the 1D valence subbands.

The magnetic field is an interesting additional parameter, since it can be applied experimentally in a well-controlled way and modifies fundamentally the electronic structure. Brum and Bastard[2] have calculated the conduction-band energy levels of quantum wires using a confinement by finite-barrier quantum wells in the x and z directions in the presence of electric and magnetic fields. Here, we present calculations of the valence-band structure and the interband absorption of 1D systems in a magnetic field. First of all, we show how the magnetic field can be incorporated into our theoretical description of the 1D states of the Γ_6 and Γ_8 bands. Then the theory is applied to the type-I and type-II wire arrays of Sec. III B of I which consist of symmetric, 10-nm-large GaAs-$Ga_{0.7}Al_{0.3}As$ quantum wells subjected to periodic modulations of the conduction- and valence-band edges in one lateral (x) direction. This model describes a variety of experimental situations. The 2D ($V_1=0$), the spatially direct 1D (large V_1, type I), the spatially indirect 1D (large V_1, type II) systems, as well as the continuum of systems between these three, are studied by varying the modulation V_1.

The electronic system is coupled in two ways to the magnetic field B. First, the quasiangular momenta and spins of the periodic Bloch functions give rise to magnetic moments that interact with B. This is described[3] by adding the "spin" terms $g^*\mu_B B m_s$ to the conduction-band Hamiltonian [Eq. (4) of I] and $2\kappa\mu_B B m_j$ to the diagonal elements of the Luttinger-Kohn Hamiltonian H_{Γ_8} [Eqs. (6) and (7) of I]. The Bohr magneton is defined by $\mu_B=e\hbar/(2m_0)$. The spin splitting of the conduction-band energies is neglected because it is usually small compared to the broadening caused by impurities and inhomogeneities in real samples. In GaAs, for instance, the effective Landé g factor $g^*=-0.445$ (from Ref. 4) leads to a splitting $g^*\mu_B B$ of only 0.26 meV at 10 T.

Second, a charged particle moving in a magnetic field is deflected by the Lorentz force. This leads to the replacement of the wave vector $\mathbf{k}$ by $\mathbf{k}'=\mathbf{k}+e\mathbf{A}/\hbar$ in the effective-mass equation for the envelope wave function. We consider a constant magnetic field $\mathbf{B}=(0,0,B)$ that is described by the vector potential $\mathbf{A}=(0,Bx,0)$ in the Landau gauge. Therefore, k_y has to be replaced by $k_y'=k_y+x\lambda^{-2}$, where the magnetic length λ is defined by $\lambda^{-2}=eB/\hbar$. We shift the origin of the coordinate system in x by $k_y\lambda^2$, so that the minimum positions of the magnetic-field-induced parabolas are fixed at $x=0$ and the off-diagonal elements of H_{Γ_8} are independent of k_y. The potential $V_x(x-k_y\lambda^2)$ becomes the only k_y-dependent term. For zero V_x, the eigenenergies are degenerate in k_y and the spectrum of eigenvalues consists of discrete Landau levels. For nonzero V_x, the position of $V_x(x)$ relative to the magnetic-field-induced parabolas matters, and the Landau levels become bands with a dispersion in k_y. When $V_x(x)$ is invariant under a translation of x_0 in the x direction [$V_x(x)=V_x(x+x_0)$], the corresponding energy dispersions are also periodic [$E(k_y)=E(k_y+x_0\lambda^{-2})$]. The hh-lh coupling in the valence band does not affect this symmetry.

We suppose that the carrier motion in the x and z directions are decoupled due to a stronger confinement in the growth (z) than in the lateral (x) direction. Our Γ_6 wave functions correspond to the lowest z-related conduction subband, while the Γ_8 wave functions $\Psi\uparrow$ and $\Psi\downarrow$

are based on the first and second heavy-hole and the first light-hole state of the quantum well in the z direction.[1]

The magnetic field in question does not lift the inversion symmetry in the z direction. The two different types of Γ_8 wave functions $\Psi\uparrow$ and $\Psi\downarrow$ remain decoupled, but the corresponding eigenenergies differ due to the "spin" terms. We expand the lateral wave functions $\varphi(x)$ on the basis of harmonic-oscillator functions

$$\varphi(x)=\sum_{n=0}^{\infty} c_n \langle x|n\rangle , \tag{1}$$

$$\langle x|n\rangle=(2^n n!\sqrt{\pi}\lambda)^{-1/2} e^{-1/2(x/\lambda)^2} H_n(x/\lambda) . \tag{2}$$

In Eq. (2) the H_n's are the Hermite polynomials. We define the following raising and lowering operators:

$$a^\dagger=\frac{\lambda}{\sqrt{2}}\left[-\partial_x+\frac{x}{\lambda^2}\right] ,$$
$$a=\frac{\lambda}{\sqrt{2}}\left[\partial_x+\frac{x}{\lambda^2}\right] , \tag{3}$$

which increase ($a^\dagger$) or decrease (a) the index of the oscillator function in the usual way and obey $[a,a^\dagger]=1$.

When projected on this basis, the conduction-band eigenvalue equation becomes

$$\sum_n \{[\hbar\omega_c(n+\tfrac{1}{2})-E]\delta_{n,m}+\langle m|V_x(x-\lambda^2 k_y)|n\rangle\}c_n=0 , \tag{4}$$

with $\omega_c=eB/m^*$. The valence-band Hamiltonian H that determines the solutions $\Psi\uparrow$ via Eq. (12) of I reads for nonzero B

$$\mathcal{H}=\begin{pmatrix} E_{\rm hh1}-\hbar\omega_{\rm hh}(a^\dagger a+\frac{1}{2}) & -\frac{\hbar^2}{\mu\lambda^2}a^2 & 0 \\ +V_x(x-\lambda^2 k_y)+3\kappa\mu_B B & & \\ -\frac{\hbar^2}{\mu\lambda^2}a^{\dagger 2} & E_{\rm lh1}-\hbar\omega_{\rm lh}(a^\dagger a+\frac{1}{2}) & \frac{\hbar^2\sqrt{2}}{m_0 l_0\lambda}a \\ & +V_x(x-\lambda^2 k_y)-\kappa\mu_B B & \\ 0 & \frac{\hbar^2\sqrt{2}}{m_0 l_0\lambda}a^\dagger & E_{\rm hh2}-\hbar\omega_{\rm hh}(a^\dagger a+\frac{1}{2}) \\ & & +V_x(x-\lambda^2 k_y)-3\kappa\mu_B B \end{pmatrix} , \tag{5}$$

where $\omega_{\rm hh}=eB/m_{\rm hh}$ and $\omega_{\rm lh}=eB/m_{\rm lh}$. The functions $\Psi\downarrow$ are described by interchanging a and $a^\dagger$ in the off-diagonal terms and reversing the signs of the "spin" terms.

The lateral potentials are supposed to be

$$V_x(x)=\pm V_1\cos\left[\frac{2\pi}{L_x}x\right]$$

for the conduction band, and (6)

$$V_x(x)=V_1\cos\left[\frac{2\pi}{L_x}x\right]$$

for the valence band. We use the same magnitude of the lateral modulation for the conduction- and valence-band edges. The negative and positive signs in Eq. (6) correspond to the type-I and type-II configurations, respectively (see Fig. 7 of I). At large V_1 the former (latter) configuration leads to electron-hole transitions that are spatially direct (indirect) in the x direction.

When the magnetic field **B** lies along the z direction, particularly interesting features arise from the competition between the modulation period L_x and the magnetic length λ. A new type of oscillation, periodic in B^{-1} but different from the Shubnikov–de Haas oscillations, has been observed in the low-temperature magnetoresistance and explained by calculations of the Landau conduction subbands of laterally modulated 2D systems.[5,6] These systems exhibit a formal similarity with ordinary superlattices subjected to a magnetic field perpendicular to the superlattice axis.[7,8]

For the matrix elements of the harmonic V_x of Eq. (6) we use the analytical expression[9]

$$\langle n|\cos[q(x-x_0)]|m\rangle = M^q_{n,m}\times\begin{cases}\cos(qx_0) & \text{for } n+m \text{ even}\\ -i\sin(qx_0) & \text{for } n+m \text{ odd} ,\end{cases} \tag{7}$$

with

$$M^q_{n,m}=\left[\frac{i\lambda q}{\sqrt{2}}\right]^{m-n}\left[\frac{n!}{m!}\right]^{1/2} e^{-\lambda^2 q^2/4} L_n^{m-n}(\tfrac{1}{2}\lambda^2 q^2)$$

for $n\le m$.

The condition $n\le m$ does not restrict the general validity, since $M^q_{n,m}=M^q_{m,n}$. The Laguerre polynomials L are defined in accordance with Ref. 10.

The parameters used in the following calculations are given in Sec. III of I, with the exception of κ, for which we take the bulk GaAs value $\kappa=1.2$ (from Ref. 4). For clarity, we discuss the energy levels and interband transitions of only one valence-band solution ($\Psi\uparrow$). The other one ($\Psi\downarrow$), although its energies and wave functions differ slightly from those of $\Psi\uparrow$, shows very much the same general behavior.

Figure 1 shows the dispersion of the lowest Landau conduction and valence subbands of the type-I array for a magnetic field B of 4 T. The lateral potential has a

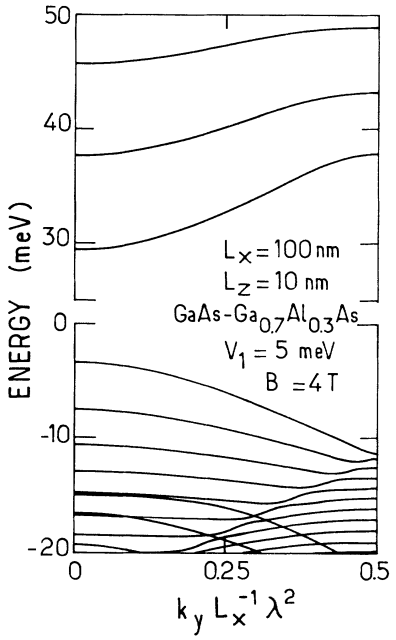

FIG. 1. Conduction-band (upper half) and valence-band (lower half) energy levels of a type-I wire array in a magnetic field B as a function of the in-wire wave vector k_y. The zero of the electron (hole) energy scale corresponds to the bottom of the Γ_6 (top of the Γ_8) band of bulk GaAs.

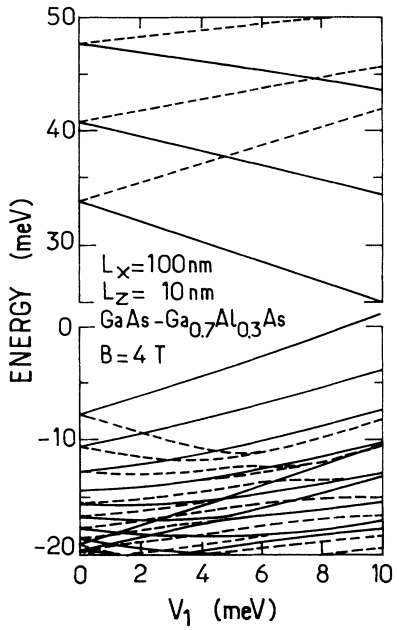

FIG. 2. Energy levels at $k_y=0$ (solid lines) and $k_y=\frac{1}{2}L_x\lambda^{-2}$ (dashed lines) of the type-I wire array in a magnetic field B as a function of the strength V_1 of the lateral potential. The energy axes are defined as in Fig. 1.

modulation V_1 of 5 meV and a periodicity L_x of 100 nm for both electrons and holes. Figure 1 describes the energy levels for any k_y, since they are invariant under a reflection at $k_y=0$ and a translation of k_y by $L_x\lambda^{-2}$. For zero k_y the potential V_x tends to localize both the electrons and the holes at the same place as do the magnetic-field-induced parabolas (at $x=0$). The energy separations decrease with $q_y=k_yL_x^{-1}\lambda^2$ increasing from 0 to 0.5 (V_x tends to localize at $x=\pm L_x/2$ for $q_y=0.5$). The anticrossings of the lh-like branches (for zero k_y at -15.0, -16.4, and -19.2 meV) with the hh branches in that energy region are small, since the corresponding Landau-level indices are very different and hence the coupling matrix elements small.

In Fig. 2 we have plotted the energies at $q_y=0$ (solid lines) and 0.5 (dashed lines) as a function of the lateral potential V_1. At $V_1=0$ the solid and dashed lines coincide and correspond to the Landau levels of the 2D electron gas in a perpendicular magnetic field. They are equally spaced in the conduction band, while in the valence band the hh-lh coupling leads to varying separations. With increasing V_1 we first deal with a discrete spectrum of Landau levels, then with a set of splitted Landau bands, and finally with a continuous spectrum of overlapping Landau bands. The lateral potential increases the dimensionality of the system in a magnetic field B from 0 to 1, in contrast to the decrease from a 2D to a 1D behavior with increasing V_1 at zero B.

In the following calculations of the magnetoabsorption, sample imperfections are modeled by a replacement of the δ function that ensures the energy conservation of the interband transition by a Gaussian function with a full width of 2 meV at $1/e$ maximum. Figure 3 shows the absorption spectrum for the 0D case ($V_1=0$, $B=4$ T). The absorption spectra for a polarization parallel to x and to y are identical. There, the transitions $h1e1$ (from the first valence to the first conduction subband) and $h2e2$ are dominant. The first lh-like ($h9e1$) transition, which shows up as a shoulder on the high-energy side of the $h2e2$ transition for a polarization in the xy plane, dominates the spectrum for a polarization parallel to z.

The absence of an anisotropy in the xy plane is not surprising. Clearly, a magnetic field in the z direction does not disturb the equivalence between the x and the y

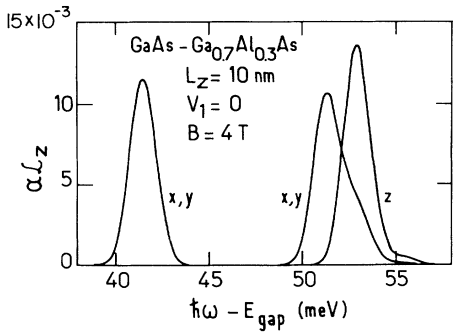

FIG. 3. Absorption $\alpha\mathcal{L}_z$ of a quantum well for a polarization in the xy plane (x,y) and parallel to the growth axis (z) in the presence of a magnetic field B. E_{gap} is the bulk GaAs band gap.

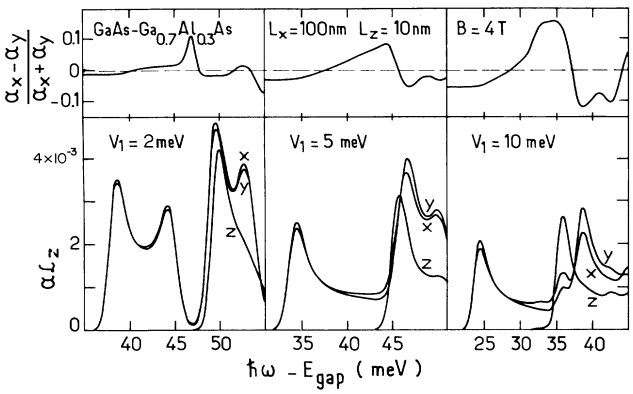

FIG. 4. Polarization-dependent absorption (lower curves) and normalized xy anisotropy (upper curves) of type-I wire arrays with different modulation V_1 of the lateral potential in a magnetic field B.

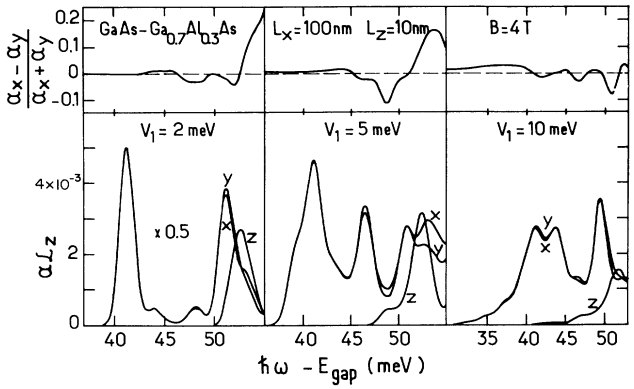

FIG. 5. Same as Fig. 4 for type-II wire arrays. The absorption curves are multiplied by a factor of 0.5 for $V_1=2$ meV.

directions existing for $V_1=0$. This results from the calculation as follows. For $V_1=0$ the oscillator functions $\langle x|n\rangle$ [Eq. (2)] are the exact conduction-band eigenfunctions [Eq. (4) has only diagonal elements]. The off-diagonal terms of the valence-band Hamiltonian $\mathcal{H}$ [Eq. (5)] couple only basis functions that exhibit different indices. Thus, a given conduction-band eigenstate $\langle x|n\rangle$ cannot have simultaneously a nonzero overlap integral with the hh and with the lh part of a valence-band eigenstate. The xy anisotropy, being proportional to the product of the two overlap integrals [$J_{\mathrm{hh1}}J_{\mathrm{lh1}}$, see Eq. (16) of I] becomes zero.

How does the lateral confinement ($V_1\neq 0$) changes the interband absorption in a magnetic field? Figure 4 summarizes the results for the lowest-energy transitions of the type-I wire array. With increasing lateral potential, the energy position and the height of the peaks in the absorption spectrum decrease. Exhibiting the shape of a 0D density of states at zero V_1, the transitions become similar to the shape of a 1D density of states with increasing V_1. For $V_1=2$ meV, the peaks of the x and y absorption at 38.5 and 44.5 meV correspond to transitions between the first electron and hole subbands ($h1e1$) at $q_y=0$ and $q_y=0.5$, respectively. The peak for the z polarization at 50 meV is due to the first lh-like transition $h7e1$ at $q_y=0$. All the transitions of Fig. 4, corresponding to either $q_y=0$ or $q_y=0.5$, can be identified by comparing their energy position with Fig. 2. The transitions at $k_y=0$ obey the same general dependence on the polarization in the xy plane as the 1D systems at $B=0$.[1] This anisotropy, which allows the identification of the hh or lh character of the participating valence subband, increases with increasing lateral potential. The absorption and anisotropy curves for $V_1=10$ meV are similar to the corresponding zero-magnetic-field results of Fig. 10 of I. By increasing V_1 from 0 to 10 meV, we continuously change a magnetic-field-controlled system into a system where the influence of the magnetic field is negligible in comparison with that of the lateral potential V_x.

Figure 5 shows the results for the type-II wire array. It follows from symmetry that this system has the subband dispersions of the type-I configuration (Fig. 1) with the electron branches reflected at $q_y=0.25$. In the same way, Fig. 2 describes the type-II system when the solid and dashed electron curves are interchanged [then, the dashed (solid) electron curves correspond to $q_y=0$ ($q_y=0.5$)]. At zero magnetic field, the transitions between the lowest conduction- and the topmost valence-band states are weak because they are strongly indirect in real space. At finite B, these transitions are forbidden by the conservation of the in-wire wave vector k_y. The fundamental absorption edge shifts barely, with V_1 increasing from 0 to 5 meV. Already the lowest allowed transition ($h1e1$) exhibits a sizeable overlap of the electron and hole wave functions. The transition extends over a smaller energy range, and its joint density of states is larger in comparison with the direct system. For V_1 increasing above 5 meV, the absorption edge shifts to lower energies, but the wave-function overlap decreases. At $V_1=10$ meV, the energy of the transition with $q_y=0.5$ equals 33 meV, as can be seen from Fig. 2 by comparing the lowest solid electron with the highest dashed hole curve. It contributes to the absorption that increases continuously with the photon energy in this range. This characteristic increase shows that the 0D spatially direct transitions of the 2D system in a magnetic field become 1D spatially indirect with increasing lateral confinement. The xy-anisotropy curves of Fig. 5 obey no simple rule.

In conclusion, we have shown how a lateral 1D modulation of increasing strength V_1 changes the shape and the xy anisotropy of a 2D system in a perpendicular magnetic field. At small V_1, the type-I configuration leads to stronger modifications than the type-II configuration. A striking consequence is the stronger absorption peak of the type-II system with respect to that of the type-I system at $V_1=2$ meV, although the former configuration spatially separates the electron and holes. Over the whole range of V_1, the xy anisotropy of the peaks of the type-I system that correspond to van Hove singularities at $k_y=0$ obeys the characteristic dependence on the hh-lh mixing derived in I.

We thank R. Ferreira for fruitful discussions. We gratefully acknowledge the support from Professor G. Abstreiter and from the Deutsche Forschungs Gemeinschaft (DFG), the Ministère de la Recherche et de la Technologie, and the Centre National d'Etude des Télécommunications.

[1]U. Bockelmann and G. Bastard, preceding paper, Phys. Rev. B **45**, 1688 (1992).

[2]J. A. Brum and G. Bastard, Superlatt. Microstruct. **4**, 443 (1988).

[3]M. Altarelli, in *Semiconductor Superlattices and Heterojunctions,* edited by G. Allan, G. Bastard, N. Boccara, M. Lannoo, and M. Voos (Springer-Verlag, Berlin, 1986).

[4]*Numerical Data and Functional Relationships in Science and Technology,* edited by O. Madelung, Landolt-Börnstein, New Series, Group III, Vol. 17, Pt. 2.10.1 (Springer-Verlag, Berlin, 1982).

[5]R. R. Gerhardts, D. Weiss, and K. v. Klitzing, Phys. Rev. Lett. **62**, 1173 (1989).

[6]R. W. Winkler, J. P. Kotthaus, and K. Ploog, Phys. Rev. Lett. **62**, 1177 (1989).

[7]A. V. Chaplik, Solid State Commun. **53**, 539 (1985).

[8]J. C. Maan, Surf. Sci. **196**, 518 (1988).

[9]F. G. Bass and I. B. Levinson, Zh. Eksp. Teor. Fiz. **49**, 914 (1965) [Sov. Phys. JETP **22**, 635 (1966)].

[10]J. S. Gradshteyn and J. M. Ryzhik, *Tables of Integral, Series and Products* (Academic, New York, 1965).